Inorg. Chem. **2005**, *44*, 546–551

$[BDTA]_2[Cu(mnt)_2]$: An Almost Perfect One-Dimensional Magnetic Material

Sarah S. Staniland,[†] Wataru Fujita,[‡] Yoshikatsu Umezono,[‡] Kunio Awaga,[‡] Philip J. Camp,[†] Stewart J. Clark,[§] and Neil Robertson*[,†]

School of Chemistry, University of Edinburgh, West Mains Road, Edinburgh EH9 3JJ, U.K., Department of Chemistry, Graduate School of Science, Nagoya University, Chikusa-ku, Nagoya 464-8602, Japan, and Department of Physics, University of Durham, South Road, Durham DH1 3LE, U.K.

Received October 30, 2004

$[BDTA]_2[Cu(mnt)_2]$ (BDTA = benzo-1,3,2-dithiazolyl, mnt = maleonitriledithiolate) was crystallized in the space group $P\bar{1}$ with an inversion center on Cu giving a stacked structure with each metal complex anion sandwiched by two cations. Short intermolecular S···S contacts give rise to a one-dimensional chain lateral to the stacking axis. Variable-temperature magnetic susceptibility and EPR measurements indicate that the salt behaves as an ideal one-dimensional Heisenberg antiferromagnetic material from 2 K $\leq T \leq$ 300 K, with a coupling constant of J/k_B = 16–17 K; the very low temperature magnetic properties are in quantitative agreement with the predictions of quantum field theory. DFT calculations are consistent with the formation of a one-dimensional magnetic chain with interstack interactions mediated by the BDTA counterions.

Introduction

Metal bis(1,2-dithiolene) complexes typically possess a square-planar, electronically conjugated system and have been studied extensively showing properties such as superconducting,[1] conducting,[2] nonlinear optical,[3] and magnetic behavior.[2] Materials based on such complexes are usually low dimensional, forming many novel systems that, in addition to providing new functional materials, advance the theoretical understanding of 1- and 2-D electronic behavior.

The low dimensionality of such materials is due to the planar structure of metal−bis(1,2-dithiolene) complexes which normally form a stacking motif, allowing electronic communication throughout the stack through a strong $\pi-\pi$ overlap between sulfur atoms in adjacent complexes. Typical counterions may segregate each stack to hinder further electronic communication.

The counterion selected is of key importance as it controls the packing and hence electronic communication that occurs between dithiolene complexes. The examples of $[NEt_4]_2$, $[NPr_4]_2$, and $[NBu_4]_2[Cu(mnt)_2]$ salts (mnt = maleonitriledithiolate) illustrate the importance of the size of the counterion. The structures of all these salts show a uniform stacks of dithiolene complexes where the stacking distance increases with the larger counterions, leading to weaker intermolecular interactions. Thus, the magnitude of intrastack exchange coupling and the conductivity both decrease on variation of the counterion in the series $[NEt_4]$, $[NPr_4]$, and $[NBu_4]$[4−6] In addition, larger counterions can interrupt the regularity of the stack and cause the dithiolenes to form dimers, leading to a nonmagnetic ground state. Thus, smaller counterions promote both the uniform stacking required for long-range magnetic order and strong intermolecular interactions between the dithiolene complexes. This is illustrated by $[NH_4][Ni(mnt)_2]\cdot H_2O$, which exhibits uniform stacking and ferromagnetic order at 4.5 K, with T_c rising by 0.4 K $kbar^{-1}$ as the intermolecular distance within the stacks is reduced further under pressure.[7,8]

The number of small counterions available for study is limited, and an alternative approach to the promotion of strong intermolecular interactions involves the use of planar

* To whom correspondence should be addressed. E-mail: neil.robertson@ed.ac.uk.
[†] University of Edinburgh.
[‡] Nagoya University.
[§] University of Durham.

(1) Cassoux, P. *Coord. Chem. Rev.* **1999**, *185*−*186*, 213.
(2) Robertson, N.; Cronin, L. *Coord. Chem. Rev.* **2002**, *227*, 93.
(3) Romaniello, P.; Lelj, F. *Chem. Phys. Lett.* **2003**, *372* (1, 2), 51.
(4) Plumlee, K. W.; Hoffman, B. M.; Ratajack, M. T.; Kannewurf, C. R. *Solid State Commun.* **1974**, *15* (10), 1651.
(5) Plumlee, K. W. Ph.D. Thesis, Northwestern University, Evanston, IL, 1975.
(6) Plumlee, K. W.; Hoffman, B. M.; Ibers, J. A.; Soos, Z. G. *J. Chem. Phys.* **1975**, *63* (5), 1926.

10.1021/ic048479+ CCC: $30.25
Published on Web 01/13/2005

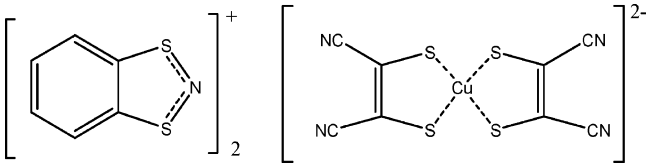

Figure 1. [BDTA]$_2$[Cu(mnt)$_2$].

counterions, as there is essentially an unlimited number of planar cations. These have given rise to other materials containing stacked metal−bis-mnt complexes that display varied and unusual magnetic properties. For example, charge-transfer salts based on pyridinium cations include [ethyl-pyridinium][Ni(mnt)$_2$][9] with ferromagnetic coupling below 50 K, [1-(4-bromo-2-fluorobenzyl)pyridinium][Ni(mnt)$_2$],[10,11] and [(1-(4- fluorobenzyl)-4-amino)pyridinium][Ni(mnt)$_2$],[12] with large 1-D ferromagnetic and antiferromagnetic interactions respectively down each [Ni(mnt)$_2$]$^-$ stack showing long-range magnetic ordering below 2 K.

Functional, planar cations have been explored to yield hybrid conducting/magnetic materials. These include (perylene)$_2$[M(mnt)$_2$] (M = Cu and Ni), with segregated stacks of anions and cations, conducting down the perylene stacks, with localized unpaired spins on the anion stacks.[13] (BDNT)$_2$-[Ni(mnt)$_2$] (BDNT = 4,9-bis(1,3-benzodithiol-2-ylidene)-4,9-dihydronaphtho[2,3-*c*][1,2,5]thiadiazole) is another hybrid material.[14] The salt was found to be conducting due to BDNT, as well as displaying a ferromagnetic interaction of the [Ni(mnt)$_2$]$^-$ anions, although the structure has not yet been determined.

Planar counterions can also lead to a hybrid system where the cations and anions form an alternately stacked motif. For example [(bis(*N*-methylphenazinium))$_2$][Cu(mnt)$_2$] forms 1-dimensional antiferromagnetic chain through an alternating stack, although the interaction is very weak as there are two stacked cations between each [Cu(mnt)$_2$] anion.[15]

In this study, we have explored a dithiazolyl counterion as a new type of planar cation within the series of [M(mnt)$_2$]$^{2-}$ salts (Figure 1). The dithiazolyl family is composed of extensive planar phenyl and N,S-hetrocyclic rings fused together. Paramagnetic examples of these have displayed interesting magnetic properties due to their delocalized systems with strong intermolecular $\pi-\pi$ interactions.[16−18] In this initial study the counterion is the diamagnetic monocation BDTA (BDTA = benzo-1,3,2-dithiazolyl) (Figure 1), chosen for its long-term solution stability allowing ready crystal growth. It has previously been studied extensively as a neutral compound since its structure is similar to known organic superconductors and displays transitions above 346 K to paramagnetic liquid, paramagnetic solid, and antiferromagnetically ordered phases.[19] BDTA is of interest as a cation as it is conjugated, planar, and stable and has large sulfur atoms that may provide S−S interaction between BDTA and [Cu(mnt)$_2$]$^{2-}$.

Experimental Section

Synthesis. [BDTA][Cl][20] and [NBu$^t_4$]$_2$[Cu(mnt)$_2$][21] were synthesized by literature methods. [BDTA]$_2$[Cu(mnt)$_2$] was prepared by layering [BDTA][Cl] in MeCN on top of [NBu$^t_4$]$_2$[Cu(mnt)$_2$] in DCM and allowing it to diffuse over 4 days. The microcrystalline bulk sample was washed with MeCN and ether and analyzed by CHN (Anal. Calcd for $C_{20}H_8CuN_6S_8$: C, 36.82; H, 1.24; N, 12.88. Found: C, 37.25; H, 1.21; N, 12.56). Powder X-ray diffraction was used to establish that the bulk sample possessed the same structure as the single crystal used to determine the structure. The bulk sample was then used for the magnetic and EPR measurements.

X-ray Crystallography Data: $C_{20}H_8CuN_6S_8$, M = 652.384; triclinic; a = 6.7870(4), b = 7.1930(4), c = 13.2820(10) Å; α = 83.347(2), β = 81.029(2), γ = 73.646(5)°; V = 612.79(7) Å^3; T = 296 K; space group $P\bar{1}$, Z = 1; μ(Mo Kα) = 1.9 mm^{-1}; 4311 reflections measured, 2621 independent reflections (R_{int} = 0.0214) which were used in all calculations. The final wR(F^2) was 0.0798. X-ray diffraction intensities were collected on a MacScience DIP-Labo 3200 imaging plate type diffractometer with Mo Kα radiation at room temperature. An absorption correction was not carried out. The structure was solved by direct methods and refined by full-matrix least squares against F^2 using all data (SHELXTL). H atoms were placed in calculated positions and allowed to ride on their parent atoms. All non-H atoms were modeled with anisotropic displacement parameters.

Magnetic Susceptibility. Magnetic susceptibility measurements were performed on a microcrystalline sample of BDTA$_2$[Cu(mnt)$_2$] from 300 to 2 K using a Quantum design MPMS$_2$ SQUID magnetometer with MPMS MultiVu Application software to process the data. The magnetic field used was 0.1 T.

EPR Analysis. Temperature-dependent EPR measurements were carried out on a JES-FA200 spectrometer in a temperature range of 4−300 K by means of a variable-temperature helium gas flow.

DFT Plane Wave Calculations. The calculations were performed using the density functional formalism within the generalized gradient approximation using the CASTEP code.[22] The electronic wave functions are expanded in a plane wave basis set up to a kinetic energy cut off of 380 eV which converges the total

(7) Allan, M. L.; Coomber, A. T.; Marsden, I. R.; Martens, J. H. F.; Friend, R. H.; Charlton, A.; Underhill, A. E. *Synth. Met.* **1993**, *56* (2−3), 3317.
(8) Coomber, A. T.; Beljonne, D.; Friend, R. H.; Bredas, J. L.; Charlton, A.; Robertson, N.; Underhill, A. E.; Kurmoo, M.; Day, P. *Nature* **1996**, *380*, 144.
(9) Robertson, N.; Bergemann, C.; Becker, H.; Agarwal, P.; Julian, S. R.; Friend, R. H.; Hatton, N. J.; Underhill, A. E.; Kobayshi, A. *J. Mater. Chem.* **1999**, *9*, 1713.
(10) Xie, J.; Ren, X.; Song, Y.; Zou, Y.; Meng, Q. *J. Chem. Soc., Dalton Trans.* **2002**, (14), 2868.
(11) Xie, J.; Ren, X.; Gao, S.; Meng, Q. *Chem. Lett.* **2002**, (6), 576.
(12) Xie, J.; Ren, X.; Gao, S.; Zhang, W.; Li, Y.; Lu, C.; Ni, C.; Liu, W.; Meng, Q.; Yao, Y. *Eur. J. Inorg. Chem.* **2003**, (13), 2393.
(13) da Gama, V.; Henriques, R. T.; Almeida, M.; Alcacer, L. *J. Phys. Chem.* **1994**, *98* (3), 997.
(14) Uruichi, M.; Yakushi, K.; Yamashita, Y.; Qin, J. *J. Mater. Chem.* **1998**, *8* (1), 141.
(15) Kuppusamy, P.; Ramakrishna, B. L.; Manoharan, P. T. *Inorg. Chem.* **1984**, *23* (24), 3886.
(16) Rawson, J. M.; McManus, G. D. *Coord. Chem. Rev.* **1999**, *189*, 135.
(17) Awere, E. G.; Burford, N.; Haddon, R. C.; Parsons, S.; Passmore, J.; Waszczak, J. V.; White, P. S. *Inorg. Chem.* **1990**, *29* (23), 4821.
(18) Barclay, T. M.; Cordes, A. W.; George, N. A.; Haddon, R. C.; Itkis, M. E.; Mashuta, M. S.; Oakley, R. T.; Patenaude, G. W.; Reed, R. W.; Richardson, J. F.; Zhang, H. *J. Am. Chem. Soc.* **1998**, *120* (2), 352.
(19) Fujita, W.; Awaga, K.; Nakazawa, Y.; Saito, K.; Sorai, M. *Chem. Phys. Lett.* **2002**, *352* (5, 6), 348.
(20) Wolmershaeuser, G.; Schnauber, M.; Wilhelm, T. *J. Chem. Soc., Chem. Commun.* **1984**, (9), 573.
(21) Dance, I. G.; Miller, T. R. *Inorg. Chem.* **1974**, *13* (3), 525.
(22) Segall, M. D.; Lindan, P. J. D.; Probert, M. J.; Pickard, C. J.; Hasnip, P. J.; Clark, S. J.; Payne, M. C. *J. Phys.: Condens. Matter* **2002**, *14* (11), 2717.

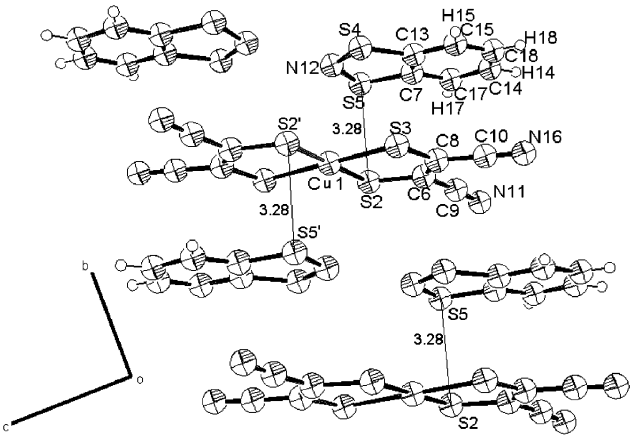

Figure 2. Crystal structure of $[BDTA]_2[Cu(mnt)_2]$ viewed along the *a* axis, with intermolecular distances (Å) smaller than the sum of the van der Waal radii (S···S = 3.6 Å) shown.

energy of the system to better than 1 meV/atom. The valence electron and ion interactions are described using ultrasoft pseudopotentials. Integrations over the Brillouin zone are performed on a grid which also converges the total energy of the system to 1 meV/atom. We have constrained the magnetic properties to investigate their relative energies: ferromagnetic and various antiferromagnetic configurations. Geometry optimizations are performed by relaxing the positions and unit cell parameters under the influence of the Hellmann−Feynman forces and stresses, respectively.

Results and Discussion

Preparation and X-ray Structure. Single crystals of $[BDTA]_2[Cu(mnt)_2]$ were prepared by slow mixing of [BDTA]Cl in MeCN with $[NBu^t_4]_2[Cu(mnt)_2]$ in a dichloromethane solution. Needle-shaped black crystals were collected after 4 days.

$[BDTA]_2[Cu(mnt)_2]$ crystallizes in the space group $P\bar{1}$ and has an inversion center on the copper atom. The structure shows an alternating, diagonal stacked system in the *b*−*c* plane, with a single $[Cu(mnt)_2]^{2-}$ anion sandwiched between two BDTA cations. Intermolecular contacts shorter than the sum of the van der Waal radii are seen between S5 on BDTA and S2 on $[Cu(mnt)_2]^{2-}$ which, along with the symmetry equivalent, creates a discreet unit of $[Cu(mnt)_2]^{2-}$ with a BDTA above and below in the *b*−*c* plane (Figure 2). Extended interactions throughout each stack are not observed as all of the other intrastack distances are large with the shortest S···S contact at 3.824 Å. Each stack however is tilted by 28.20° out of the *a*−*b* plane, allowing short intermolecular contacts along the *a* axis, between a $[Cu(mnt)_2]^{2-}$ anion and the adjacent BDTA cations. An S···S short intermolecular interaction is seen from S5 on BDTA to S3 and S2′ on $[Cu(mnt)_2]^{2-}$ in the adjacent stack (intermolecular distances of 3.418 and 3.397 Å, respectively). Thus, the discreet units within each stack in the *b*−*c* plane form S···S interactions along the *a* axis and allow a chain of contacts to form (Figure 3). There are no other intermolecular distances small enough to provide significant interactions, and a 1-dimensional chain is observed.

EPR Studies. Electron paramagnetic resonance (EPR) studies were performed on the solid sample at variable temperatures from 4 to 300 K. The spectrum has a principle feature at $g = 2.022$, with small positive peaks at lower fields that can be assigned to parallel and perpendicular *g* values, respectively. However, the smaller peaks are poorly resolved and further discussion will focus on the principle peak. The line width and $g_{||}$ value for each temperature were plotted (Figure 4). Both the line width and $g_{||}$ values decrease with temperature to a negative peak at 10 K and then increase again at lower temperatures. The value of $g_{||}$ ranges from 2.016 to 2.022, and the line width, from 6.31 to 7.79 mT. At room temperature $g_{||} = 2.022$, which is comparable with literature values obtained for other $[Cu(mnt)_2]^{2-}$ complexes. $[NMP]_2[Cu(mnt)_2]$ has $g_{av} = 2.043$,[15] and $[NBu_4]_2[Cu(mnt)_2]$ has $g_{av} = 2.047$.[23] All these values are seen to be greater than the free electron value of $g_e = 2.0023$, as Cu^{2+} has a more than half filled orbital configuration.[24] The deviation of *g* from the free electron value for such $[Cu(mnt)_2]^-$ species is small, however, indicating that a large proportion of the electron density is delocalized across the complex.[25] In comparison, $[NH_4]_2[CuCl_4]$ has most of the spin density on the metal and has a value of $g_{av} = 2.109$, deviating much more significantly from g_e.

Over the temperature range studied the value of *g* and the line width have a small variation of 0.0058 and 1.48 mT, respectively. A lattice of anisotropic magnetic centers will show a large shift at the ordering temperature, and the small shift in *g* value observed indicates that the anions can be considered as possessing approximately isotropic Heisenberg spins.[26] The decreasing values that occur with reduced temperature can be ascribed to demagnetization[27,28] as well as the fact that the copper center is not perfectly isotropic. The value of *g* at low temperatures increases again as magnetic ordering is achieved. The shape of the line width versus temperature curve concurs with reported 1-D and quasi 1-D antiferromagnets.[29−31] Thus, the EPR data show that the copper center is an approximately Heisenberg spin center with electron density delocalized across the ligand and that magnetic ordering occurs around 10 K.

Magnetic Susceptibility. The molar magnetic susceptibility is presented in Figure 4 as a function of temperature. It was confirmed that, at a temperature $T = 2$ K, the magnetization increased linearly with applied magnetic fields in the range $0\ T \le B \le 5\ T$. The temperature-dependent magnetic susceptibility was fitted with the theoretical susceptibility of an $S = {}^1/_2$ isotropic Heisenberg chain. The

(23) Teschmit, G.; Strauch, P.; Barthel, A.; Reinhold, J.; Kirmse, R. *Inorg. Chim. Acta* **2000**, *298* (1), 94.
(24) Basu, P. *J. Chem. Educ.* **2001**, *78* (5), 666.
(25) Goodman, B. A.; Raynor, J. B. *Adv. Inorg. Chem. Radiochem.* **1970**, *13*, 135.
(26) Jacobs, I. S.; Bray, J. W.; Hart, H. R., Jr.; Interrante, L. V.; Kasper, J. S.; Watkins, G. D.; Prober, D. E.; Bonner, J. C. *Phys. Rev. B* **1976**, *14* (7), 3036.
(27) Kittel, C. *Introduction to Solid State Physics*, 6th ed.; Wiley: Chichester, New York, 1986; Vol. 1, p 346.
(28) Stanger, J.-L.; Andre, J.-J.; Turek, P.; Hosokoshi, Y.; Tamura, M.; Kinoshita, M.; Rey, P.; Cirujeda, J.; Veciana, J. *Phys. Rev. B* **1997**, *55* (13), 8398.
(29) Oshikawa, M.; Affleck, I. *Phys. Rev. Lett.* **1999**, *82* (25), 5136.
(30) Ohta, H.; Imagawa, S.; Ushiroyama, H.; Motokawa, M.; Fujita, O.; Akimitsu, J. *J. Phys. Soc. Jpn.* **1994**, *63* (8), 2870.
(31) Okuda, K.; Hata, H.; Date, M. *J. Phys. Soc. Jpn.* **1972**, *33* (6), 1574.

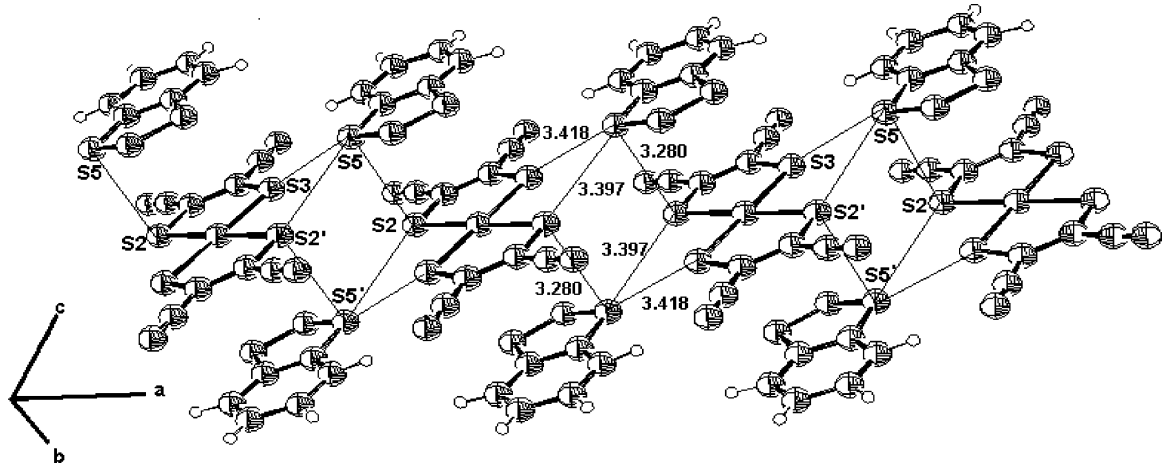

Figure 3. Crystal structure of $BDTA_2[Cu(mnt)_2]$ viewed to show interactions along the *a* axis. Intermolecular distances (Å) smaller than the ionic radii (S···S = 3.6 Å) are shown.

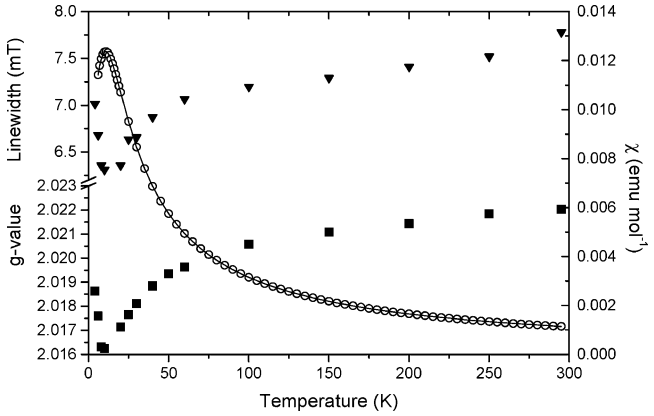

Figure 4. Magnetic properties of $[BDTA]_2[Cu(mnt)_2]$ as functions of temperature: *g* value (■) and line width (▼) from variable-temperature EPR studies; molar magnetic susceptibility, χ, from experiments (○) and as fitted by the Bonner−Fisher model (eq 1) with $J/k_B = (16.718 \pm 0.068)$ K (—).

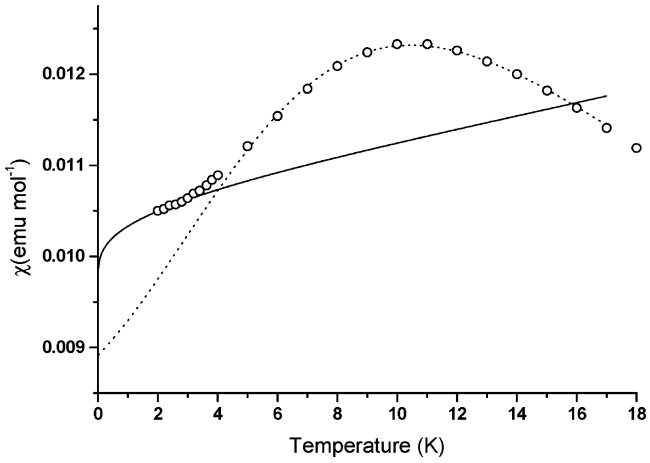

Figure 5. Magnetic susceptibility, χ, of $[BDTA]_2[Cu(mnt)_2]$ in the temperature range 0 K < *T* < 18 K: experimental results (○); Bonner−Fisher curve (eq 1) with $J/k_B = (16.165 \pm 0.055)$ K (---); exact low-temperature curve (eq 2) with $J/k_B = (15.4 \pm 2.0)$ K (—).

spin Hamiltonian for this system is given by $H = J\Sigma_i \mathbf{S}_i \cdot \mathbf{S}_{i+1}$, where $J > 0$ is the exchange coupling constant and $\mathbf{S}_i$ is the spin on site *i*. The original calculations were due to Bonner and Fisher,[32] who considered chains and rings of up to 11 spins and then extrapolated to the bulk limit. This procedure yielded accurate results for $k_BT > 0.5J$ but was less reliable at lower temperatures where the spin−spin correlation length exceeds the dimensions of the systems considered. A useful closed-form expression for the Bonner−Fisher results was put forward by Estes et al.[33] and is given by

$$\chi(T) = \frac{Ng^2\mu_B^2}{k_BT}\left(\frac{0.25 + 0.14996x + 0.30094x^2}{1 + 1.9862x + 0.6885x^2 + 6.0626x^3}\right) \quad (1)$$

where $x = J/2k_BT$ and *N* is the number of spins. According to eq 1, the peak in the magnetic susceptibility occurs at $T_{max} = 0.6475J/k_B$ and has height $\chi(T_{max}) = 0.1468Ng^2\mu_B^2/J$. Note that the Bonner−Fisher calculations are expected to be reliable in the region of the peak. Fitting the experimental results over the temperature range 5 K < *T* < 300 K gave $J/k_B = (16.718 \pm 0.068)$ K, $T_{max} = (10.825 \pm 0.044)$ K, and $\chi(T_{max}) = (0.01253 \pm 0.00055)$ emu mol^{-1}. The position of the peak is consistent with the ordering temperature obtained from the EPR measurements.

In Figure 5 we show the magnetic susceptibility in the temperature range 0 K < *T* < 18 K. We performed a fit in this restricted temperature range using eq 1, which yielded $J/k_B = (16.165 \pm 0.055)$ K; the deviation between this value and that obtained from fitting in the range 5 K < *T* < 300 K is only 3% and, therefore, insignificant. It can be seen in Figure 5 that an extrapolation of eq 1 does not fit the experimental data below 5 K. This was to be anticipated because of the small systems considered by Bonner and Fisher; at low temperatures the spin−spin correlation length will exceed the dimensions of the finite-size systems considered, rendering the extrapolation to the bulk limit extremely hazardous. Using quantum field theory, Eggert et al. have derived the *exact* asymptotic scaling behavior of the magnetic susceptibility in the limit $T \rightarrow 0$ K.[34] The central result is

(32) Bonner, J. C.; Fisher, M. E. *Phys. Rev. A* **1964**, *135* (3A), A640.
(33) Estes, W. E.; Gavel, D. P.; Hatfield, W. E.; Hodgson, D. J. *Inorg. Chem.* **1978**, *17* (6), 1415.

$$\chi(T) \approx \chi(0)\left[1 + \frac{1}{2\ln(T_0/T)}\right] \quad (2)$$

where $T_0 \approx 7.7J/k_B$ and $\chi(0) = Ng^2\mu_B{}^2/J\pi^2$ is the exact zero-temperature value of the subsceptibility;[35,36] note that this model predicts a divergent slope at $T = 0$ K. In combination with the Bonner−Fisher model, the ratio of the peak and zero-temperature susceptibilities is given by $\chi(T_{max})/\chi(0) = 0.1468\pi^2 = 1.449$. The result of Eggert et al. has been shown to be very useful in describing the low-temperature susceptibility of Sr_2CuO_3, which behaves like an almost perfect one-dimensional Heisenberg antiferromagnet with $J/k_B \approx 1700$ K.[37] Fitting eq 2 to the experimental results for $[BDTA]_2[Cu(mnt)_2]$ in the range 0 K < T < 3 K yields $\chi(0) = (0.00935 \pm 0.000048)$ emu mol^{-1}, $J/k_B = (15.4 \pm 2.0)$ K, and $\chi(T_{max})/\chi(0) = 1.340 \pm 0.059$. As shown in Figure 5, the observed low-temperature susceptibility exhibits a "crossover" from eq 1 to eq 2; the agreement between the respective fit parameters shows that the magnetic behavior of $[BDTA]_2[Cu(mnt)_2]$ is consistent with that of an almost perfect one-dimensional Heisenberg antiferromagnet. This indicates that the magnetic chains within the material are well segregated from one another.

The magnetic interaction within $[BDTA]_2[Cu(mnt)_2]$ of $J/k_B = (16.718 \pm 0.068)$ K is surprisingly large compared with other intermolecular, nonbonded magnetic interactions. The crystal structure of the salt suggests that the magnetic exchange pathway lies along the *a* axis and is communicated through a long pathway involving the nonmagnetic cation as well as the dithiolene ligand. An example of a material that displays magnetic exchange mediated through a nonmagnetic counterion is $NH_4Ni(mnt)_2{\cdot}H_2O$[7,8] with 3-D ferromagnetic order at $T_c = 4.5$ K. In this example, magnetic exchange between $[M(mnt)_2]^{x-}$ through nonmagnetic cations appear to give rise to interactions of a few kelvin. However, the antiferromagnetic exchange constant for $[BDTA]_2[Cu(mnt)_2]$ of $J/k_B = (16.718 \pm 0.068)$ K is significantly larger.

Side-by-side interactions are unusual in metal dithiolene salts, where strong interactions occur more typically within stacks. However, side-by-side interactions have been reported for [BEDT-TTF][Ni(dmit)$_2$] (BEDT-TTF = bis(ethylenedithio)tetrathiafulvalene, dmit = 1,3-dithiol-2-thione-4,5-dithiolate),[38] which was found to have semiconducting properties communicated by interaction between [BEDT-TTF] molecules, transverse to the alternate stack. Although side-by-side interaction are usually considered to be weak, in this example the calculated overlap integrals in the material showed that the interaction between BEDT-TTF molecules was over twice as large in the lateral direction than in the stacking direction.

DFT Calculations. Plane-wave DFT calculations were carried out on the title system with varying restraints on the magnetic structure. A 1-D antiferromagnetic ground state with the chain lying in the stacking direction was compared with a 1-D antiferromagnetic ground state with side-by-side interactions along the *a* axis. It was found that the *a* axis 1-D chain gave a lower energy by 0.2 meV, consistent with our analysis of the short intermolecular contacts in the X-ray structure which lie in this direction. In turn the system was restrained to yield a ferromagnetic ground state and comparison showed the antiferromagnetic ground state was lower in energy than the ferromagnetic ground state by 1.0 meV. This latter value is expressed as 12 K when divided by the Boltzmann constant, and remarkably it can be seen to have not only the same sign but also the same order of magnitude as the measured magnetic exchange coupling of $J = 16-17$ K. Previous publications have used DFT methods with a Gaussian basis set to predict values of coupling constants within isolated binuclear[39] and polynuclear[40] transition-metal compounds, showing good correlation with the trends and sign of coupling constants. Also, plane-wave DFT methods have been applied to conducting molecular materials[41] and continuous-lattice systems such as bulk metals.[42] We are not aware, however, of previous application of plane-wave DFT methods to the rationalization of magnetic properties and estimation of coupling constants within extended-lattice molecular magnetic materials, and it is interesting to note the apparent success of the method in reproducing and rationalizing the empirical results in this case. This suggests that such methods may show a general utility in related examples and their potential should be more widely explored.

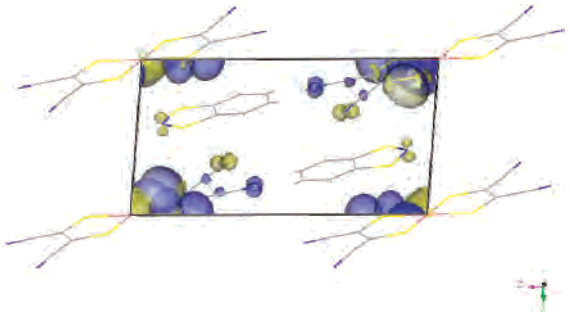

Figure 6. Spin density distribution within the unit cell determined by DFT methods. The spin density on the N atom of the cation can be clearly seen. Electron density isosurfaces are set at ±0.005 e/Å^3.

The proposed coupling mechanism that involves an exchange pathway via the BDTA counterion suggests that some nonzero spin density should be observed on the BDTA units. The calculated spin density within the unit cell is shown in Figure 6 and indicates spin density located principally on the nitrogen atom of the BDTA cation, corresponding to a 0.011 electron difference. Although no significant spin density was determined on the sulfur atoms of the BDTA, the observation of any spin density at all on

(34) Eggert, S.; Affleck, I.; Takahashi, M. *Phys. Rev. Lett.* **1994**, *73* (2), 332.
(35) Griffiths, R. B. *Phys. Rev.* **1964**, *133*, A768.
(36) Yang, C. N.; Yang, C. P. *Phys. Rev.* **1966**, *150* (1), 327.
(37) Eggert, S. *Phys. Rev. B* **1996**, *53* (9), 5116.
(38) Kobayashi, H.; Kato, R.; Kobayashi, A.; Sasaki, Y. *Chem. Lett.* **1985**, (2), 191.
(39) Ruiz, E.; Cano, J.; Alvarez, S.; Alemany, P. *J. Comput. Chem.* **1999**, *20* (13), 1391.
(40) Ruiz, E.; Rodriguez-Fortea, A.; Cano, J.; Alvarez, S.; Alemany, P. *J. Comput. Chem.* **2003**, *24* (8), 982.
(41) Rovira, C.; Novoa, J. J.; Mozos, J.-L.; Ordejon, P.; Canadell, E. *Phys. Rev. B* **2002**, *65* (8), 1723.
(42) Cocula, V.; Starrost, F.; Watson, S. C.; Carter, E. A. *J. Chem. Phys.* **2003**, *119* (15), 7659.

this molecule indicates that it is able to play a role in the magnetic properties of the material and lends weight to the proposed coupling pathway. The calculations also indicate that much of the spin density within the metal complexes is located on the sulfur atoms and this is consistent with the observation of a relatively large magnetic coupling despite the large distance between copper centers in the material and also with the low hyperfine coupling constant shown in the EPR experiment. In summary, the DFT calculations fully support both the observation of an antiferromagnetic ground state with $J = 16-17$ K and also the proposal that the 1-D Heisenberg chain forms through unusual counterion-mediated, side-by-side magnetic interaction of metal dithiolene complexes.

Conclusions

[BDTA]$_2$[Cu(mnt)$_2$] has been synthesized and structurally characterized. It was found to behave as an ideal 1-dimensional Heisenberg antiferromagnetic material from $2 \leq T \leq 300$, with a magnetic coupling constant of $J/k_B = 16.718 \pm 0.068$ K obtained from the Bonner−Fisher model. The data from 2 to 3 K were fit to the Eggert model, which better accounts for the low temperature behavior, with $J/k_B = 15.4 \pm 2$ K, in agreement with the value above. EPR studies confirmed the approximately isotropic nature of the magnetic copper center and the temperature of the magnetic ordering.

The structure is found to be an alternately stacked system in the $b-c$ plane. Inspection of the X-ray structure suggests that magnetic exchange is propagated along the a axis through the chain of dithiolene complexes via the nonmagnetic BDTA cation. Although the pathway between magnetic centers is unconventional and long, a relatively strong interaction is observed, attributed to the large side-by-side interaction between the sulfur atoms on the anion and cation. These conclusions were supported by the use of plane-wave DFT computational methods which gave a good estimate of the sign and magnitude of J and also suggested a side-by-side exchange pathway involving some spin density on the BDTA counterions.

Acknowledgment. We thank the EPSRC and the University of Edinburgh for financial support.

IC048479+